Hindawi

Research Article

Heat Index Based Optimisation of Primary Process Parameters in Friction Stir Welding on Light Weight Materials

Stephen Leon Joseph Leon,[1] N. Manikandan [iD],[2] R. Santhanakrishnan,[3] Mohsin O. Al-Khafaji,[4] Hayder Mahmood Salman,[5] Harishchander Anandaram,[6] R. Malkiya Rasalin Prince,[7] L. Karthick [iD],[8] and R. Rajesh Sharma [iD][9]

[1]*Engineering Department, University of Technology and Applied Sciences-Ibri, Ibri, Oman*
[2]*Department of Mechanical Engineering, SRM Institute of Science and Technology, Ramapuram, Chennai, India*
[3]*School of Engineering and Technology, CMR University, Bengaluru, Karnataka, India*
[4]*Air Conditioning and Refrigeration Techniques Engineering Department, Al-Mustaqbal University College, Babylon 51001, Iraq*
[5]*Department of Computer Science, Al-Turath University College, Al Mansour, Baghdad, Iraq*
[6]*Centre for Excellence in Computational Engineering and Networking, Amrita Vishwa Vidyapeetham, Coimbatore, India*
[7]*Department of Mechanical Engineering, Karunya Institute of Technology and Sciences, Coimbatore, India*
[8]*Department of Mechanical Engineering, Hindusthan College of Engineering and Technology, Coimbatore, India*
[9]*Adama Science and Technology University, Nazrēt, Ethiopia*

Correspondence should be addressed to R. Rajesh Sharma; sharmaphd10@gmail.com

In friction stir welding, tool shoulder diameter and its rotational speed are the major influencing parameters than others. A simple novel correlation is proposed to select the optimum range of tool shoulder diameter with respect to the chosen rotational speed and vice versa. The conditions to apply derived correlation were defined through process heat index number as the joint efficiency in the friction stir welding depends on the effective heat supply to the volume of material deformed in the stir zone. Weld speed is the key parameter through which generated heat can be regulated towards optimum heat supply to attain defect-free weld in the stir zone. Effective heat input also has obvious effect on grain growth and corresponding property eradication in the heat affected zone. The experimental study was carried out on AA2024-T3 plates to understand the effect of process heat index on the prescribed optimum range of tool shoulder and rotational speed defined in the correlation. Eventually, a novel relationship was attained between the first order process influencing parameters to deliver maximum joint efficiency.

1. Introduction

Friction stir welding is the most preferable solid state joining technique for several high strength-to-weight ratio materials like aluminium alloys. In this welding, high-strength recrystallised metal structure weld joints are formed without cracking defects as the entire joining process is carried out above the recrystalisation temperature and below the melting point [1]. On the other hand, when the process is carried out in a temperature lower than the recrystallisation temperature, it results in defects like voids and tunnels in the stir zone [2], while higher process temperature leads to other defects, such as pores and flashes [2]. This indicates that the process parameters should be selected to induce optimum heat supply to ensure the entire joining process to be carried out in the temperature range, which produces a defect-free weld joint. Tool/matrix contact surface area and the relative velocity between the tool and the matrix are responsible for heat generation during this joining process (Figure 1).

Being major influencing factors of heat generation, appropriate selection of tool rotation speed and traverse speed can optimise heat generation rate in friction stir
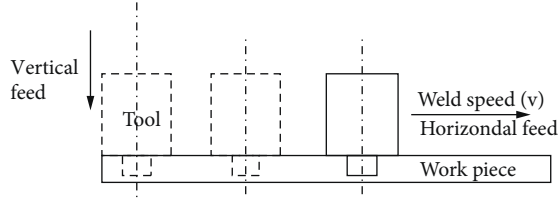
FIGURE 1: Tool movement at various stages.

welding [3]. Apart from this, contact conditions along the tool/matrix interface is also a major influencing factor on the effective heat supply [4]. Among all the heat supply boundaries, the tool shoulder/matrix is the major contributor in total heat generation. In order to optimise the heat generation rate, appropriate selection of shoulder diameter with respect to the tool rational speed and traverse speed is highly recommended.

Many researchers have tried to optimise tool shoulder diameter with respect to pin diameter, tool rotation speed, and welding speed [5–7]. These researches concluded an optimum shoulder diameter on the basis of constrained input parameter limits. For instance, even though the proven optimal tool shoulder pin ratio is 3, the combined effect of low tool rotational speed and high welding speed resulted in weld defects due to insufficient heat supply [8]. This reveals that the geometrical tool dimensions cannot be optimised without considering the tool rotation as well as welding speed.

The simplest way of optimising shoulder diameter with respect to the chosen process parameters is through the analysis of maximum utilisation of available torque. Arora et al. [9] developed a new criterion to optimise shoulder diameter on the basis of maximum utilisation of available torque. Nandan et al. [10] proposed a model which reveals that excess tool rotational speed or excess tool shoulder diameter leads to excess softening of material along the tool/matrix contact interface. This leads to poor mixing of material along the weld line and causes weld defects. Apart from this, it leads to excess material spill out on the top surface of the weldment, leading to excess flash weld defect. From this, it can be understood that there is always need for a simple correlation that can reveal the basic information for the selection of shoulder diameter range with respect to the tool rotational speed, and vice versa. Although the welding speed is an important factor to be considered in the estimation of effective heat supply during the joining process, its effect on heat generation is less comparing with the tool rotational speed. Many researchers [11–13] optimised weld speed with respect to the thickness and other properties on the workpiece to be joined. In this paper, a simple novel correlation is proposed to select the optimum range of tool shoulder diameter with respect to the chosen rotational speed and vice versa. The obtained correlation was related with the heat index value to attain to relate primary process parameters with other process conditions like absolute thermal resistance of the base metal. Derived conditions were validated through experimental analysis.

2. Optimum Values

The maximum utilisation of available torque depends on the design of appropriate tool geometry. The amount of heat generation in the tool/matrix interface depends on the friction between the contact surfaces. Friction in turn depends on the local velocity difference between the rotating tool and metal flow, which is quantified by the slip rate (δ) given by [14]

$$\delta = \exp\left[-\frac{E_{eff}}{E_{max}}\right], \tag{1}$$

where the ratio between effectively transferred energy (E_{eff}) and maximum available energy (E_{max}) is termed as transfer efficiency.

If $E_{eff} = E_{max}$ then $T_{max} = T_s$ [14].

Assuming 90% transfer efficiency.

$E_{eff} = 0.9 E_{max}$ then the minimum attainable slip rate $\delta_{min} = 0.4$.

The slip rate can also be estimated by [15]

$$\delta = 0.3 \exp\left[\frac{\omega r}{1.87}\right] - 0.026, \tag{2}$$

where r is the radial distance from the axis to the point at which slip rate is to be estimated.

Substituting $\delta_{min} = 0.4$ in Equation (2), the maximum value of,

$$\omega r = 0.59. \tag{3}$$

Local heat generation analysis done by the Schmidt et al. [13] recorded maximum heat generation at the shoulder edge of the tool. It indicates that δ_{min} is achieved at the point where $r = R_{Shoulder}$. So Equation (3) can be rewritten as,

$\omega R_{shoulder} = 0.59$ in which optimum energy transfer can be achieved.

Although Equation (3) gives a minimum optimum value of shoulder radius, during the welding stage, for higher welding velocity, the heat generated by the optimum shoulder radius may not be sufficient. The obtained optimum values by Arora et al. [9] reveal that sliding and sticking torque increase with an increase in shoulder diameter. In a particular diameter, the total toque developed is equally shared by sliding and sticking. Beyond that, the sticking torque reduces, and the sliding torque increases with a further increase in shoulder diameter. In other words, at a particular diameter for a given tool rotational speed, when the slip factor is 0.5, sticking torque reaches its maximum value and the maximum value of shoulder radius can be optimised at this limit.

Applying the conditions, equation (3) can be rearranged for its maximum value as,

$$\omega R_{Shoulder} = 1.05. \tag{4}$$

So depending on the forward motion of the tool per rotation, the required heat index value changes, and based on the required heat index value, the value of $\omega R_{Shoulder}$ should be opted in the range of 0.59 to 1.05.

2.1. Least Values. Equations (3) and (4) explain the range of the combined values of the tool shoulder and its rotational velocity. These two factors individually have their lower limits, which cannot be reduced beyond that. Every researcher tried to reduce the values of R_{shoulder} and ω to improve the property eradication in thermo-mechanically affected zone (TMAZ) as these two factors are directly proportional to the heat supply. Too much reduction in these two parameters leads to improper material flow around the tool pin and results in weld defects in the stir zone (SZ). A coupled thermal/material flow model developed by Hamilton et al. [14] suggests that

$$\text{Maximum effective strain rate} \, \dot{\varepsilon} = \frac{R_{\text{Shoulder}} \sqrt{6}\omega}{3h}. \quad (5)$$

Here, h refers to the workpiece thickness.

Equation (5) reveals that when $R_{\text{shoulder}} = 1.2\,h$, effective strain equals the tool rotational velocity and it reduces to its minimum value at the tool pin tip. From this, it can be understood that R_{shoulder} should always be more than 1.2 times of workpiece thickness to ensure proper material flow till its extreme depth of the Stir zone.

Minimum tool rotational speed can be explained using the required effective heat input during the process. Peak temperature during the process can be expressed as [15]

$$\frac{T_{\max}}{T_m} = K \left(\frac{\omega^2}{10^4 v} \right)^{\gamma}. \quad (6)$$

Here, T_m is the melting temperature of the material, v is the weld speed, and K and γ are coefficients suggested by Chen et al. [15].

When $T_{\max} = T_{\text{sat}} \approx 0.9\,T_m$ temperature-dependent yield strength of the parental metal becomes the minimum value, and it can be considered as extreme condition in frictional heat generation during the joining process. And for the extreme values of K and γ,

$$\text{Minimum heat index (HI)} = \frac{\omega 2}{104 v} = 20.89. \quad (7)$$

Considering all, optimum range can be written as,

$$\omega R_{\text{SHoulder}} = 0.59 \, to \, 1.05 \left| \begin{array}{l} R_{\text{Shoulder}} \geq 1.2h \\ HI \geq 20.89 \end{array} \right. . \quad (8)$$

2.2. Model Consistency with Literature Data. From the previous studies, it is evident that an increase in shoulder diameter increases the heat generation rate. But the effective heat flux delivered to the workpiece depends on process variables like rotational speed and welding speed. Apart from these process variables, temperature-dependent material properties like yield strength, which is responsible for the flow stress, have a direct impact on effective heat supply. Variation in yield stress results in a nonuniform slip factor throughout the tool/matrix interface. This reveals that, even though the heat generation increases with an increase in shoulder diameter, it attains a saturation point where the slip factor attains its

maximum value as temperature-dependent flow stress of material that plays a significant role in self-limiting heat generation in friction stir welding. This reveals that, even though the heat generation increases with an increase in shoulder diameter, it attains a saturation point where the slip factor attains its maximum value. Figure 2 illustrates experimental results on optimum shoulder radius done on various ranges of tool rotational speed and tool shoulder radius [7, 16–19–21]. [22–25] On these results, optimum values are concluded based on the microstructure and mechanical property analysis of the joined work pieces. It can be observed that, concluded optimum values on their findings corresponding to their opted tool rotational speed are within the suggested maximum and minimum range. Experiments carried out by Padmanaban et al. [7] did not observe any considerable change in the post-weld microstructure with the change in shoulder diameter. It clearly indicates that the increase in the shoulder radius beyond the suggested maximum value ($\omega R_{shoulder} = 1.05$) does not make any difference in the weld quality.

2.3. Minimum Heat Index. Effective heat input during the joining process has an obvious effect on grain growth and property eradication in the heat affected zone. Reducing heat input beyond a limit leads to poor material flow under the tool shoulder in the stir zone and results in wormhole as well as tunnel defects. To attain a defect-free weld, the torque developed by the tool shoulder on the top tool/matrix contact surface should be sufficient to overcome the flow resistance given by the material on the bottom most surface. Reducing the yield strength of the material is a unique way to improve material flow in the stir zone. As the material yield strength is a temperature-dependent property (Figure 3), selection of the minimum possible heat index with respect to the optimum process peak temperature will result in a defect-free weld in the stir zone and improve post-weld property in the heat affected zone.

Extracted values from Figure 3 suggest that the peak temperature should be maintained at 78% of its melting point in order to reduce the yield strength of the base metal (AA2024-T3) to its lowest value [24]. From this, it can be concluded that the lowest possible operating temperature during the friction stir welding of AA2024-T3 is $0.78\,T_m$. Reducing temperature lower than $0.78\,T_m$ may lead to the insufficient material flow in the stir zone.

From Equation (6), when $T_{\max} = 0.78 T_m$, HI = 2.68.

The selection of process conditions that deliver a heat index of 2.68 is sufficient to develop a maximum flow in the stir zone for the plates with negligible thickness. For thin AA2024-T3 plates, this analytically estimated minimum heat index value (2.68) is closely aligned with the experimental results obtained by Fu et al. [25]. In their experiment, friction stir welding done on 1.6 mm thickness AA2024-T3 plates delivered its maximum joint efficiency when the heat index value was 2.45. The above condition is valid for thin plates, whereas for thick plates, the temperature gradient in the stir zone depends on the thermal resistance and the lowest temperature can be obtained by
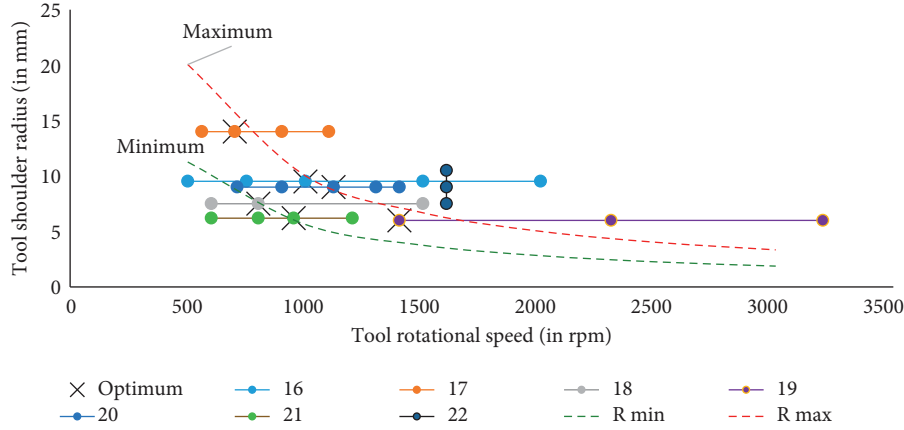
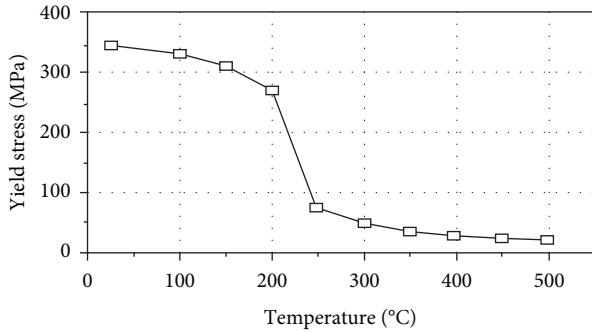Figure 2: Optimum shoulder radius obtained through different experiments.

Figure 3: Yield strength of AA2024-T3 at different temperature [21].

$$T_{\max} = \left(R_\theta Q_{eff} \right) - T_{\min}. \qquad (9)$$

Here, absolute thermal resistance $R_\theta = h/k$ for a unit cross-sectional area of the base metal. Being far away from the heat input boundary, the minimum temperature under the tool shoulder can be expected in the interface of the stir zone and the thermo-mechanically affected zone at the bottom surface of the workpiece. From Equation (9), it can be understood that the minimum heat index value depends on thermal resistance in the stir zone and the opted heat index value for the process to rise the peak temperature ($T_{\max}$) along the top contact surface should be sufficient to rise the temperature at the bottom surface ($T_{\min}$) equal to the critical temperature at which the base metal material loses its yield strength completely to facilitate the material flow. For the given absolute thermal resistance of the base metal, in order to define the required heat index conditions for the proposed "$R_{shoulder}\omega$" range in Equation (8), thermal history during the joining process with respect to the weld speed (v) has to be analysed.

3. Experimental Steady

AA2024-T3 plates of 6 mm thick were used as the base metal for the current experimental studies. Experimentally attained yield and ultimate strength of base metal properties are listed in Table 1. Process parameters used in the joining process are given in (Table 2). Tool pin diameter is kept

Table 1: Properties of base metal (AA2024-T3).

Property	Values
Thermal conductivity (W/mK)	151
Yields strength (MPa) (obtained through tensile test)	343
Ultimate strength (MPa) (obtained through tensile test)	457
Saturation temperature (°C)	510

Table 2: Levels of process variables for friction stir welding on AA2024-T3.

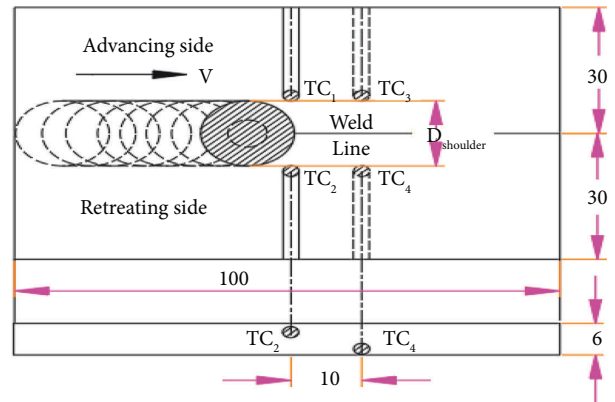| Parameter	Levels
Shoulder radius (mm)	7.5, 9, 10.5, & 12
Tool rotation speed (rpm)	800, 900, 1000, 1100, & 1200
Weld speed (mm/min)	60, 70, & 80
Tool pin shape	Cylindrical
Tool pin radius (mm)	3
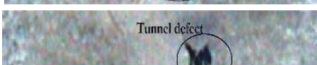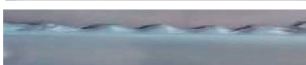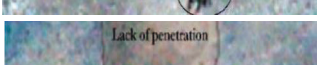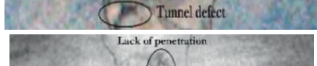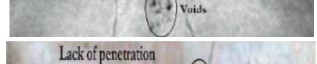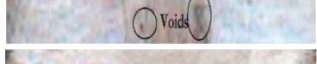
Figure 4: Experiment layout.

constant and tool shoulder diameter is increased in such a way that the ratio between tool shoulder and pin diameters are 2.5, 3, 3.5, and 4. Maximum temperature rise during the welding stage was recorded using K-type thermocouples embedded inside the drilled holes at approximately 2 mm distance for the top and bottom surfaces at different locations as shown in Figure 4. In view of considering the minor deviation in the temperature rise on advancing and

TABLE 3: Defects identified.

$R_{\text{shoulder}}\omega$	Heat index	Weld defects due to insufficient heat supply	$R_{\text{shoulder}}\omega$	Heat index	Weld defects due to excess heat supply (excess flash)
0.63	8.00	Tunnel defect	1.51	24.00	
0.75	8.00	Tunnel defect	1.51	20.57	
0.63	9.14	Tunnel defect	1.38	20.17	
0.71	10.13	Tunnel defect	1.26	16.67	
0.75	9.14	Lack of penetration / Tunnel defect	1.32	24.00	
0.88	8.00	Lack of penetration / Voids	1.21	20.17	
0.85	10.13	Lack of penetration / Voids	1.10	16.67	
0.79	12.50	Voids	1.13	24.00	

retreating sides, average values of temperature recorded by the thermocouples TC_1 and TC_2 were considered for the top surface, and average values of TC_3 and TC_4 were considered for the bottom surface. Macrostructure analysis was carried out to analyse the quality of the weld joint. Defects identified on different trails are given in Table 3.

4. Results and Discussions

4.1. Thermal Analysis. Comparing Table 3 and Figure 5, it can be concluded that the temperature gradient in the stir zone has an obvious influence over weld defects. Weld defects due to insufficient material flow were recorded when the bottom surface temperature was lesser than 410°C (equal to $0.78T_m$). The levels of defects were increasing from small voids to tunnels when the lowest temperature in the stir zone was reduced further. The lowest temperature of 374.3°C was recorded for the heat index value of 8 on the usage of the 7.5 mm shoulder radius tool. It indicates that even though $R_{\text{shoulder}}\omega = 0.63$ which is well within the recommended optimal range (Equation (8)), the chosen heat index value was not sufficient to overcome the absolute thermal resistance given by the base metal to rise the temperature of the material more than $0.78T_m$ at the bottom surface. On the other hand, surface defects developed by the excess heat supply were not identified in the top surface in the optional range of $R_{\text{shoulder}}\omega$ (0.59 to 1.05) even though the heat index value is maximum (20.89). From this, it can be concluded that irrespective of base metal thickness, defects due to excess heat supply can be avoided if the operating conditions match the recommended values in Equation (8). And also it is evident that for thin plates, the derived condition in Equation (8) is valid to obtain a defect-free weld joint even in

the lowest recommended heat index value (2.68) as thermal resistance is negligible. For thicker plates, the optimal range of $R_{\text{shoulder}}\omega$ should be related to the heat index in order to consider the effect of absolute thermal resistance to attain the minimum heat index value which can provide a defect-free weld joint. Figure 4 explains the variation in the temperature at the bottommost surface of the workpiece with respect to the temperature rise at the top surface for a 6 mm thick AA2024-T4 plate. From the extracted values of temperatures using the best curve fit method, the relationship between the temperatures at the top and bottom surfaces can be expressed as

$$T_{\max} = 0.9551 T_{\min} + 27.358. \tag{10}$$

From this Equation, it can be understood that a minimum of 419°C should be maintained at the top surface of the workpiece to ensure a $0.78T_m$ temperature at the bottom surface that shall enhance sufficient material flow to attain a defect-free joint.

4.2. Quantitative Analysis. Although the qualitative analysis with respect to the recorded thermal history provides a path to attain a defect-free weld, quantitative analysis is the unique way to optimise process parameters towards maximum joint strength. Joint strength was quantitatively analysed using the Vickers hardness test and tensile test. Obtained yield strength results for every trail are listed in Table 4. The ultimate strength of every specimen collected from different trails was compared with the ultimate strength of the base metal (Table 1) to estimate its joint efficiency. The lowest hardness value observed on every trail and corresponding joint efficiency are compared in Figure 6.
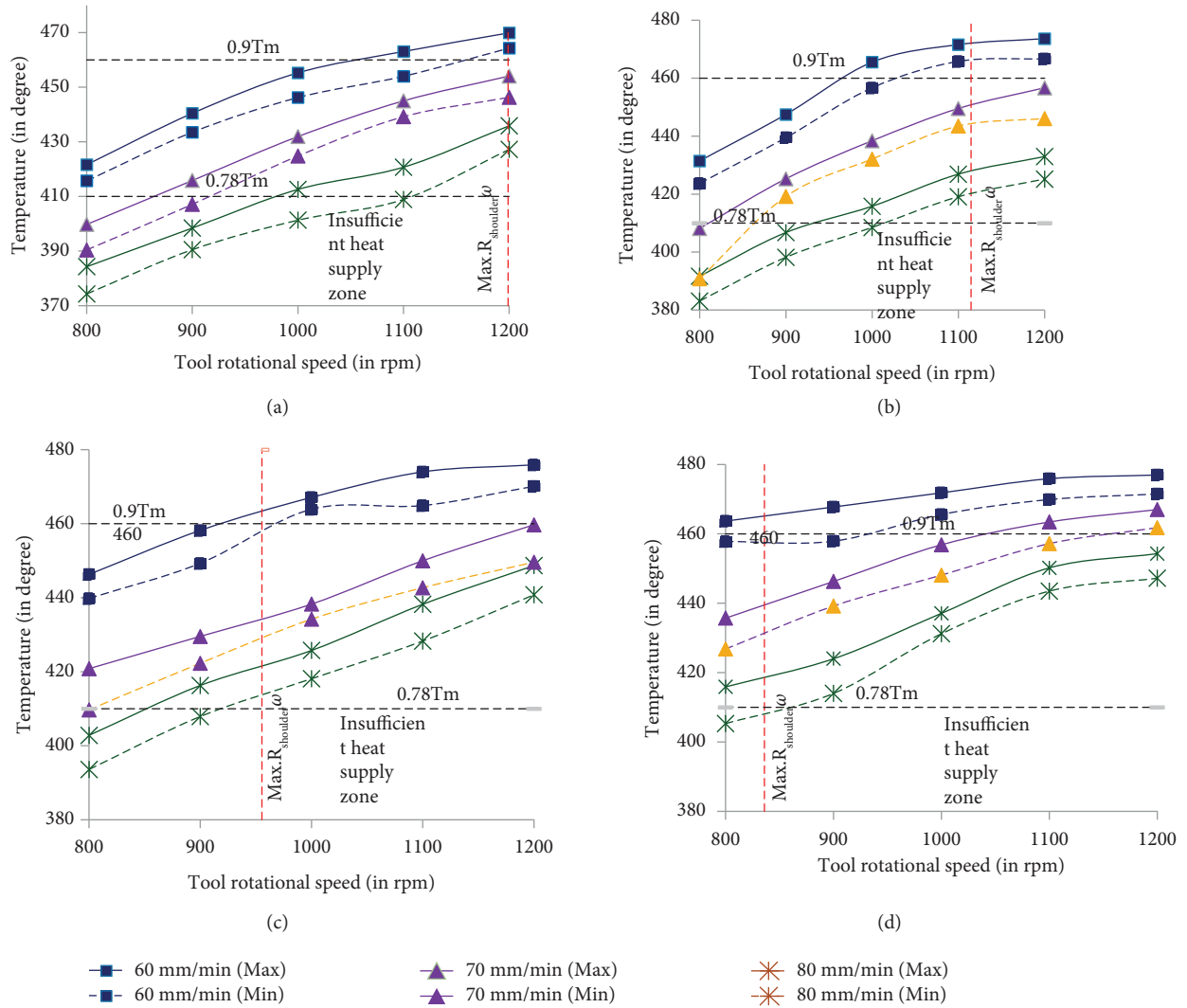
(a)

(b)

(c)

(d)

■— 60 mm/min (Max)   ▲— 70 mm/min (Max)   ✳— 80 mm/min (Max)
■- - 60 mm/min (Min)   ▲ 70 mm/min (Min)   ✳ 80 mm/min (Min)

FIGURE 5: Temperature recorded at the top and bottom surfaces during the welding stage. (a) $R_{shoulder} = 7.5$ mm; (b) $R_{shoulder} = 9$ mm; (c) $R_{shoulder} = 10.5$ mm; (d) $R_{shoulder} = 12$ mm.

TABLE 4: Experimental results on mechanical property (yield strength in MPa).

Shoulder radius	Tool rotational speed (rpm)	Weld speed		
		60 mm/min	70 mm/min	80 mm/min
	800	311.2	286.7	278.9
	900	303.2	300.8	287.3
7.5	1000	300.1	308.3	296.7
	1100	297.3	305.6	297.1
	1200	294.9	301.9	308.3
	800	308.8	287.4	284.7
	900	305.1	311.4	295.5
9	1000	299.5	307.2	299.2
	1100	299.3	303.5	312.8
	1200	296.3	302.1	312.1
	800	307.1	313.1	294.6
	900	300.9	311.9	313.1
10.5	1000	295.5	305.9	312.4
	1100	293.3	301.3	308.1
	1200	292.9	300.1	304.1

TABLE 4: Continued.

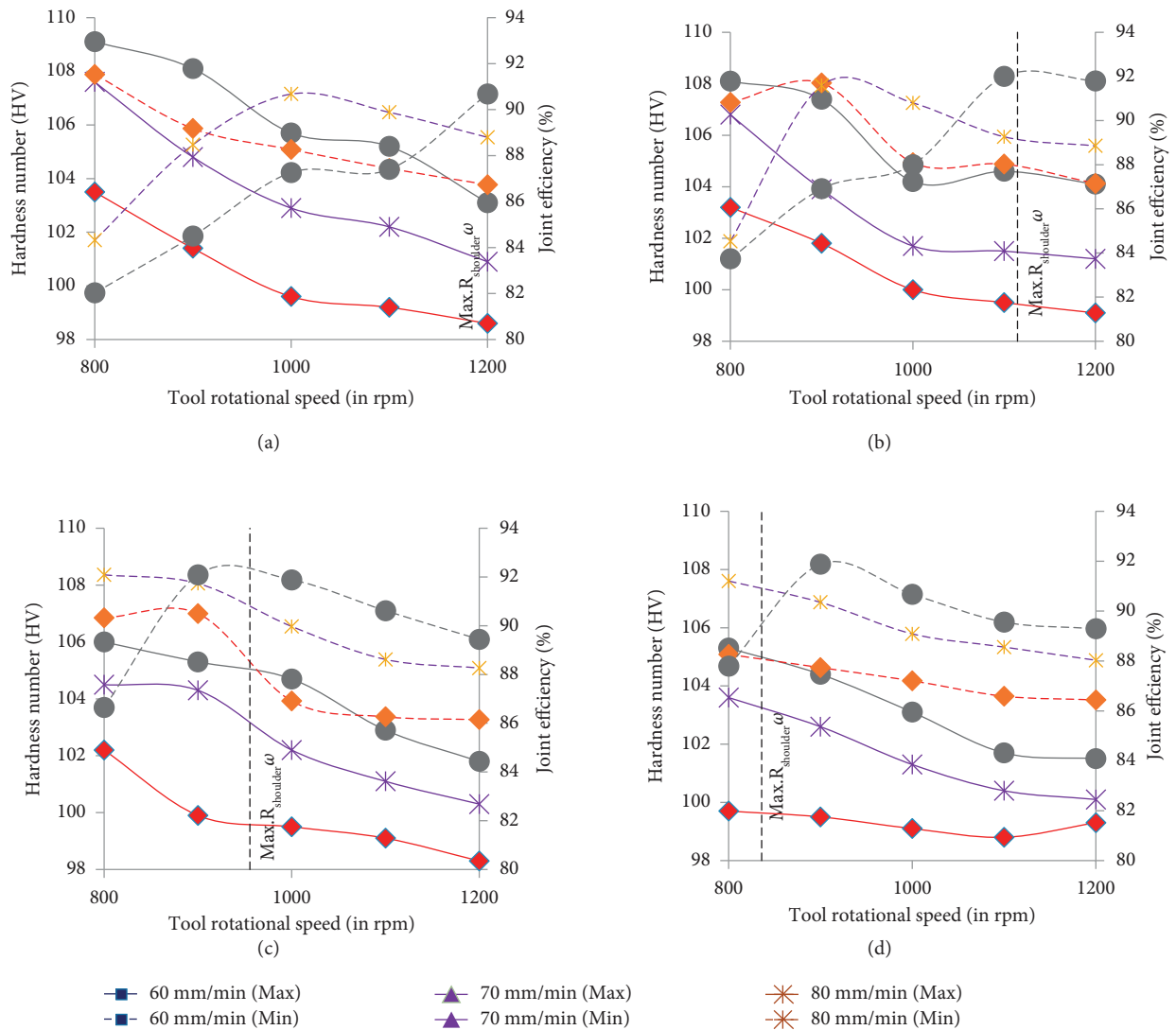| Shoulder radius	Tool rotational speed (rpm)	Weld speed		
		60 mm/min	70 mm/min	80 mm/min
	800	300.1	310.1	298.5
	900	298.3	307.2	312.4
12	1000	296.5	302.9	308.3
	1100	294.4	301.1	304.5
	1200	293.9	299.3	303.6

FIGURE 6: Joint efficiency and lowest hardness value. (a) $R_{shoulder} = 7.5$ mm; (b) $R_{shoulder} = 9$ mm; (c) $R_{shoulder} = 10.5$ mm; (d) $R_{shoulder} = 12$ mm.

As expected, the lowest hardness of 99.2 was recorded while using a 7.5 shoulder diameter tool as the heat generation rate is very low. Input heat flux is a function of relative motion between the tool and the base metal. An increase in tool rotational speed with respect to the tool feed could lead to recrystalisation of material, which in turn alters the hardness value of the base metal in the heat affected zone. As expected, the attained lowest hardness values on each trail in Figure 6 indicate that the decrease in hardness value is a direct function of tool rotational speed and the indirect function of weld speed. In a simplified form, it can be concluded that the increase in heat index value reduces the hardness value as higher heat input induces grain growth and leads to property eradication in the heat-affected zone.

From Figure 6, it can be understood that joint efficiency is a direct function of hardness value when the $R_{shoulder}\omega > 1.05$, whereas in the optimal range (from 0.59 to 1.05), the relationship between the lowest hardness value and the joint
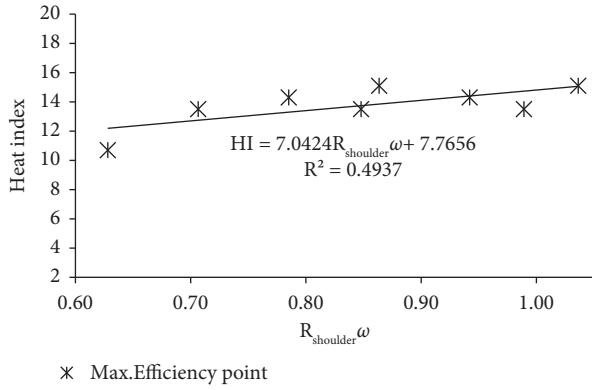
Figure 7: Heat index for the chosen tool shoulder radius and rotational speed.

efficiency is irregular due to the weld defect in the stir zone. Higher weld speed reduces the process heat index value. Even though trials done with low heat index pacified recrystallisation of material in the heat affected zone, it led to weld defects caused by insufficient heat supply in the stir zone (Table 3). It is also understood that the lowest heat index value at which defect-free weld can be obtained for the chosen "$R_{shoulder}\omega$" is the optimal value towards maximum joint efficiency as it reduces property eradication in the heat affected zone.

4.3. Optimisation of Heat Index Conditions. Tool shoulder radius and rotational speed are the key parameters to be considered to optimise total heat generation during friction stir welding. However, weld speed is the deciding factor for effective heat supply during the joining process to build a comfortable thermal environment in the stir zone to induce sufficient material flow. With the proper selection of weld speed, total heat generated can be regulated towards the optimum heat supply to attain better joint strength. From the qualitative and quantitative analysis, it is understood that process parameter optimisation can be done by relating "$R_{shoulder}\omega$" value with the heat index to define the optimum process peak temperature which could overcome the absolute thermal resistance in the stir zone and deliver a defect-free joint.

Figure 7 reveals the maximum efficiency points for the chosen key parameters. Using the best curve fit, the relationship between heat index and "$R_{shoulder}\omega$" to facilitate an amiable environment to achieve maximum joint efficiency for the prescribed circumstance can be expressed as

$$\text{Heat index} = 7.0424 R_{shoulder}\omega + 7.7656. \qquad (11)$$

This equation relates all key parameters toward maximum joint strength based on the process needs. The heat index in Equation (11) denotes the effective heat supply during the process as it indicates the number of tool rotations per one millimeter forward movement and $R_{shoulder}\omega$ defines the total heat generation controlling parameters. Here, the term "$R_{shoulder}\omega$" decides the total heat generation during the process, and the selection of the prescribed heat

index value regulates the heat supply to achieve better joint efficiency. This derived equation defines the heat index value for the prescribed "$R_{shoulder}\omega$" optimal range from 0.6 to 1.05 (equation (8)). For higher tool shoulder radius and rotational speed, the volume of material to be deformed on each revolution is higher and hence the required heat index value increases. The obtained conditions in equation (8) define the optimal conditions for heat generation, and equation (11) leads towards the optimal heat index to facilitate an amiable thermal environment based on the total heat generation.

5. Conclusions

A correlation is proposed to relate the optimum range of tool shoulder radius with respect to its rotational speed. Correlation was optimised to avoid property eradication in TMAZ and a possible selection of the least shoulder radius was obtained to ensure effective strain rate at its maximum depth in SZ. Further possible minimum value of tool rotational speed was attained through the effective heat index value to avoid surface defects. Prescribed correlation and conditions were examined through friction stir welding on AA2024-T3 plates. Based on the obtained results, the following were concluded:

(i) Obtained correlation is valid as the maximum joint efficiency is observed well within the recommended range in the correlation. There was a gradual decrease in joint efficiency when $R_{shoulder}\omega$ was greater than 1.05, irrespective of the weld speed.

(ii) Weld defects were identified at higher weld speeds when the $R_{shoulder}\omega$ value is lesser than 1.05 and the intensity of defect was increasing with a further decrease in $R_{shoulder}\omega$ value. On the other hand, excess flash defects were identified at lower weld speeds. The optimum weld speed range to attain defect-free weld was defined by the heat index number, and it was found that the maximum heat index number should not exceed 20.67.

(iii) It was identified that the minimum heat index number to be maintained according to the absolute thermal resistance of the base metal to facilitate the required effective heat supply to the volume of material to be deformed in the stir zone. Minimum heat index number was identified as 2.68 for thin AA2024-T3 plates and a correlation was obtained for thicker plates to estimate the minimum process temperature to be maintained to attain a defect-free weld in the view of relating the minimum heat index with the process peak temperature.

(iv) A novel relationship is achieved between the heat index and "$R_{shoulder}\omega$" to facilitate an amiable environment to achieve maximum joint efficiency for the prescribed circumstance.

Data Availability

The data used to support the findings of this study are included in the article. Should further data or information be

required, these are available from the corresponding author upon request.

Conflicts of Interest

The authors declare that they have no conflicts of interest regarding the publication of this paper.

Acknowledgments

References

[1] M. M. Mijajlovic, N. T. Pavlovic, S. V. Jovanovic, D. S. Jovanovic, and M. D. Milcic, "Experimental studies of parameters affecting the heat generation in friction stir welding process," *Thermal Science*, vol. 16, no. suppl. 2, pp. S351–S362, 2012.

[2] S. Bocchi, G. D'Urso, and C. Giardini, "The effect of heat generated on mechanical properties of friction stir welded aluminum alloys," *International Journal of Advanced Manufacturing Technology*, vol. 112, no. 5-6, pp. 1513–1528, 2021.

[3] A. S. Sedmak, R. Kumar, S. Chattopadhyaya et al., "Heat input effect of friction stir welding on aluminium alloy AA 6061-T6 welded joint," *Thermal Science*, vol. 20, no. 2, pp. 637–641, 2016.

[4] D. M. Veljic, B. L. Medjo, M. P. Rakin, Z. M. Radosavljevic, and N. S. Bajic, "Analysis of the tool plunge in friction stir welding - comparison of aluminium alloys 2024 T3 and 2024 T351," *Thermal Science*, vol. 20, no. 1, pp. 247–254, 2016.

[5] S. W. Park, T. J. Yoon, and C. Y. Kang, "Effects of the shoulder diameter and weld pitch on the tensile shear load in friction-stir welding of AA6111/AA5023 aluminum alloys," *Journal of Materials Processing Technology*, vol. 241, pp. 112–119, 2017.

[6] F. Sarsilmaz, "Relationship between micro-structure and mechanical properties of dissimilar aluminum alloy plates by friction stir welding," *Thermal Science*, vol. 22, no. Suppl. 1, pp. S55–S66, 2018.

[7] G. Padmanaban and V. Balasubramanian, "Selection of FSW tool pin profile, shoulder diameter and material for joining AZ31B magnesium alloy – an experimental approach," *Materials & Design*, vol. 30, no. 7, pp. 2647–2656, 2009.

[8] S. A. Khodir and T. Shibayanagi, "Friction stir welding of dissimilar AA2024 and AA7075 aluminum alloys," *Materials Science and Engineering: B*, vol. 148, no. 1-3, pp. 82–87, 2008.

[9] A. De Arora, A. De, and T. DebRoy, "Toward optimum friction stir welding tool shoulder diameter," *Scripta Materialia*, vol. 64, no. 1, pp. 9–12, 2011.

[10] R. Nandan, G. Roy, T. Lienert, and T. Debroy, "Three-dimensional heat and material flow during friction stir welding of mild steel," *Acta Materialia*, vol. 55, no. 3, pp. 883–895, 2007.

[11] C. Hamilton, S. Dymek, and A. Sommers, "A thermal model of friction stir welding in aluminum alloys," *International Journal of Machine Tools and Manufacture*, vol. 48, no. 10, pp. 1120–1130, 2008.

[12] Q. Li and M. Lovell, "On the critical interfacial friction of a two-roll CWR process," *Journal of Materials Processing Technology*, vol. 160, no. 2, pp. 245–256, 2005.

[13] H. B. Schmidt and J. H. Hattel, "Thermal modelling of friction stir welding," *Scripta Materialia*, vol. 58, no. 5, pp. 332–337, 2008.

[14] C. Hamilton, M. Kopyściański, O. Senkov, and S. Dymek, "A coupled thermal/material flow model of friction stir welding applied to Sc-modified aluminum alloys," *Metallurgical and Materials Transactions A*, vol. 44, no. 4, pp. 1730–1740, 2013.

[15] Y. Chen, H. Ding, J. z. Li, J. w. Zhao, M. j. Fu, and X. h. Li, "Effect of welding heat input and post-welded heat treatment on hardness of stir zone for friction stir-welded 2024-T3 aluminum alloy," *Transactions of Nonferrous Metals Society of China*, vol. 25, no. 8, pp. 2524–2532, 2015.

[16] X. Cao and M. Jahazi, "Effect of tool rotational speed and probe length on lap joint quality of a friction stir welded magnesium alloy," *Materials & Design*, vol. 32, pp. 1–11, 2011.

[17] M. Fazel-Najafabadi, S. F. Kashani-Bozorg, and A. Zarei-Hanzaki, "Joining of Cp-Ti to 304 stainless steel using friction stir welding technique," *Materials & Design*, vol. 31, no. 10, pp. 4800–4807, 2010.

[18] H. Fujii, L. Cui, M. Maeda, and K. Nogi, "Effect of tool shape on mechanical properties and microstructure of friction stir welded aluminum alloys," *Materials Science and Engineering A*, vol. 419, no. 1-2, pp. 25–31, 2006.

[19] H. Khalatbari and I. Lazoglu, "Friction stir incremental forming of polyoxymethylene: process outputs, force and temperature," *Materials and Manufacturing Processes*, vol. 36, no. 1, pp. 94–105, 2021.

[20] H. Nami, H. Adgi, M. Sharifitabar, and H. Shamabadi, "Microstructure and mechanical properties of friction stir welded Al/Mg2Si metal matrix cast composite," *Materials & Design*, vol. 32, no. 2, pp. 976–983, 2011.

[21] A. R. Cisko, J. B. Jordon, R. L. Amaro et al., "A parametric investigation on friction stir welding of Al-Li 2099," *Materials and Manufacturing Processes*, vol. 35, no. 10, pp. 1069–1076, 2020.

[22] J. Stephen Leon, G. Bharathiraja, and V. Jayakumar, "Analytical and experimental investigations of optimum thermomechanical conditions to use tools with non-circular pin in friction stir welding," *The International Journal of Advanced Manufacturing Technology*, vol. 107, no. 11, pp. 4925–4937, 2020.

[23] J. Stephen Leon and V. Jayakumar, "Effect of tool shoulder and pin cone angles in friction stir welding using non-circular tool pin," *Journal of applied and computational mechanics*, vol. 6, no. 3, pp. 554–563, 2020.

[24] S. S. Sabari, S. Malarvizhi, and V. Balasubramanian, "Influences of tool traverse speed on tensile properties of air cooled and water cooled friction stir welded AA2519-T87 aluminium alloy joints," *Journal of Materials Processing Technology*, vol. 237, pp. 286–300, 2016.

[25] R. D. Fu, J. F. Zhang, Y. J. Li, J. Kang, H. J. Liu, and F. C. Zhang, "Effect of welding heat input and post-welding natural aging on hardness of stir zone for friction stir-welded 2024-T3 aluminum alloy thin-sheet," *Materials Science and Engineering: A*, vol. 559, pp. 319–324, 2013.